Surface spin instabilities in the Heisenberg ferromagnet*

C. Demangeat† and D. L. Mills
Department of Physics, University of California, Irvine, California 92717
(Received 1 April 1976)

We examine the nature of the spin order in the surface of a semi-infinite Heisenberg magnet. When both ferromagnetic and antiferromagnetic exchange couplings are present, and the ground-state spin configuration of the bulk is ferromagnetic, we find the spin arrangement in and near the surface can be more complex in nature. A magnetic analog of surface reconstruction occurs. For the (100) surface of an fcc crystal with nearest-neighbor ferromagnetic and next-nearest-neighbor antiferromagnetic exchange in the bulk, we present detailed studies of the surface spin arrangements. The possibility that the exchange interactions in the surface may differ from those in the bulk is taken into account. A stability diagram for the ground state is constructed through study of the excitation spectrum of surface spin waves. For a selected set of parameters, we present results of a mean-field-theory description of the dependence of the surface spin configuration on temperature and external magnetic field.

I. INTRODUCTORY REMARKS

There is a considerable theoretical literature on the surface properties of magnetic materials. With the exception of the few papers cited below, it is generally presumed that in the surface, the spin configuration has the same nature as that of the bulk material. That is to say, if a material is ferromagnetic in the bulk, it is assumed that the spins in the surface are ferromagnetically aligned also, although the order parameter and response functions appropriate to the surface region differ from the bulk.

It is not obvious that the surface spin configuration need be the same as that of the bulk. Indeed, in an earlier paper,[1] it has been pointed out that if the surface exchange interactions are antiferromagnetic in sign while those in the bulk are ferromagnetic, then magnetic analog of the phenomenon of surface reconstruction occurs. The surface spins order in an arrangement with lower symmetry than the bulk, and the unit cell of the surface layer of spins is larger than that of a layer of ferromagnetically aligned spins in the bulk. A brief discussion of surface spin instabilities in the surface of a simple cubic ferromagnetic with antiferromagnetic surface exchange has also been presented by Wolfram and de Wames.[2]

It seems unlikely that the surface exchange can differ in sign from that in the bulk, although this might happen in the europium chalcogenides where the sign of the exchange in the bulk is a sensitive function of distance between magnetic ions.[3] In the model considered in Ref. 1, only nearest-neighbor exchange interactions were included. Blandin[4] has suggested that if the nearest-neighbor exchange is ferromagnetic, but there is appreciable antiferromagnetic next-nearest-neighbor exchange, then even when the surface exchange interactions are unchanged from their bulk values, the ferromagnetic arrangement may be unstable in the surface, while the bulk is ferromagnetic. The idea is that in some surface configurations, a surface spin has a larger ratio of next-nearest neighbors to nearest neighbors than a bulk spin. Blandin illustrated his suggestion by considering a square two-dimensional lattice of spins that cover a half plane.

Blandin's suggestion leads to the possibility that the phenomenon of magnetic surface reconstruction may be a more-common phenomenon than one would suspect from the model used by Trullinger and Mills.[1] The purpose of the present paper is to explore this question for a semi-infinite fcc lattice of spins with nearest- and next-nearest-neighbor exchange. We construct a stability diagram of the ground state, for the case where the exchange interactions in the surface differ in value from the bulk. We find surface spin reconstruction for a rather wide range of parameters. In particular, in line with Blandin's suggestion, surface spin reconstruction can occur even when the surface exchange is the same as in the bulk. After we construct the stability diagram for the ground state by searching for soft-surface spin waves,[1,4] we use a mean-field theory to examine the dependence of the surface spin arrangement on temperature and magnetic field.

In Fig. 1, we illustrate schematically the possible arrangements of the surface spins, for a (100) surface of an fcc lattice. In Fig. 1(a), the spin arrangement is what one finds in the surface when the ferromagnetic configuration is stable. In Fig. 1(b), one of the reconstructed arrangements is illustrated. As one moves from the surface into the bulk, the angle θ decreases to zero within a few atomic layers. As the temper-

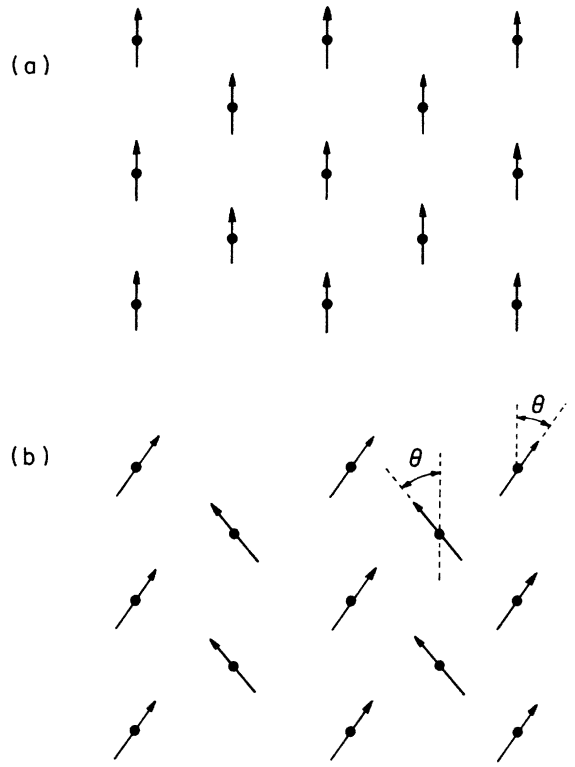

FIG. 1. Surface spin configuration in the Heisenberg ferromagnet (a) when the ferromagnetic arrangement is stable in the surface and (b) in one of the reconstructed surface spin configurations.

ature is raised, θ decreases, and we find that θ approaches zero below the bulk ordering temperature. That is, we find a temperature T_s smaller than the bulk Curie temperature T_C and one has $\theta(T)=0$ for $T_s< T< T_C$.

The work in Ref. 1 and the present study is motivated, in part, by the anomalous magnetic field dependence of the spin polarization of electrons photoemitted from EuO and other related compounds.[5] The spin polarization of electrons emitted from a clean surface fails to saturate in high fields as expected, and as observed in EuS. It has been suggested[5] that a paramagnetic layer of surface spins is responsible for this behavior. Such a region must be confined to the outermost atomic layer or two, since adsorption of Cs on the surface allows the spin polarization to saturate with magnetic field.[6] We do not believe a paramagnetic surface layer can be present at the low temperatures used in the experimental studies, and we suggest that the kind of magnetic reconstruction described here may provide a magnetic surface structure that is responsible for the effect. Unfortunately, it is very difficult for us to make quantitative or even qualitative contact with the photoemission data, so this suggestion must be regarded as tentative.

In Sec. II, we discuss the surface-spin-wave study, and the mean-field theory is presented in Sec. III.

II. SURFACE-SPIN-WAVE DISPERSION RELATION AND SOFT-SURFACE SPIN WAVES

In this paper, we shall confine our attention to the (100) surface of an fcc lattice of spins. This is the geometry appropriate to the photoemission studies cited in Sec. I. We suppose that in the bulk, the spins are coupled by nearest-neighbor exchange interactions J_1 and next-nearest-neighbor exchange J_2. In the numerical calculations, we shall always presume J_1 is ferromagnetic in sign, and J_2 antiferromagnetic in sign, or zero. This is appropriate for the ferromagnetic europium chalcogenide compounds EuS and EuO. Furthermore, we shall allow the exchange constants within the surface layer to differ in magnitude (and possibly in sign) from their bulk values. The spins in the surface are coupled by nearest-neighbor exchange $J_1^{(s)}$ and next-nearest-neighbor exchange $J_2^{(s)}$. Note that this model has as special cases both the situation discussed by Blandin ($J_2^{(s)}=J_2$, $J_1^{(s)}=J_1$) and also that discussed by Trullinger and Mills ($J_2=J_2^{(s)}=0$, $J_1>0$, $J_1^{(s)}<0$). We remark that Blandin examined a semi-infinite two-dimensional sheet of spins, while here we consider a semi-infinite three-dimensional crystal.

In previous papers, methods for studying surface spin waves have been discussed.[7] We present a summary of the theory for the fcc lattice with a (100) surface here, since the nature of the soft surface wave eigenvector will play a crucial role in the discussion of Sec. III; we shall see that the reconstructed spin configuration has the nature of a "frozen-in" surface spin wave of macroscopic amplitude.

If $J(\vec{l},\vec{l}+\vec{\delta})$ is the strength of the exchange interaction between the spin on site $\vec{l}$ and that on $\vec{l}+\vec{\delta}$, and $S^+(\vec{l})=S_x(\vec{l})+iS_y(\vec{l})$, in the spin-wave approximation $S^+(\vec{l})$ obeys the equation of motion (in units with $\hbar=1$)

$$i\frac{dS^+(\vec{l})}{dt}=S\sum_{\vec{\delta}}J(\vec{l},\vec{l}+\vec{\delta})[S^+(\vec{l})-S^+(\vec{l}+\vec{\delta})], \tag{2.1}$$

or with $S^+(\vec{l})\sim\exp(-i\Omega t)$ with Ω the spin-wave frequency,

$$\Omega S^+(\vec{l})=S\sum_{\vec{\delta}}J(\vec{l},\vec{l}+\vec{\delta})[S^+(\vec{l})-S^+(\vec{l}+\vec{\delta})]. \tag{2.2}$$

We apply the equations to the fcc crystal with

(100) surface described above. The surface is normal to the z axis, and the x and y axes are oriented as in Fig. 1, i.e., the nearest neighbors with a plane parallel to the surface are located at $\frac{1}{2}a_0(\pm\hat{x}\pm\hat{y})$. We seek solutions of Eq. (2.2) with the form

$$S^+(l_x l_y l_z) = e^{i(k_x a_0/2)l_x} e^{i(k_y a_0/2)l_y} S(l_z), \quad (2.3)$$

where l_x and l_y are integers that label sites within the planes parallel to the surface. The surface layer is $l_z = 0$.

Then for a bulk spin ($l_z \geq 2$), the amplitude $S(l_z)$ obeys

$$\begin{aligned}\Omega S(l_z) = {} & \mathcal{J}_0(\vec{k}_\parallel) S(l_z) \\ & - \mathcal{J}_1(\vec{k}_\parallel)[S(l_z+1) + S(l_z-1)] \\ & - \mathcal{J}_2(\vec{k}_\parallel)[S(l_z+2) + S(l_z-2)],\end{aligned} \quad (2.4)$$

where $\vec{k}_\parallel = \hat{x}k_x + \hat{y}k_y$, and the coefficients are

$$\begin{aligned}\mathcal{J}_0(\vec{k}_\parallel) = {} & 2S[6J_1 + 3J_2 \\ & - 2J_1 \cos(\tfrac{1}{2}k_x a_0)\cos(\tfrac{1}{2}k_y a_0) \\ & - J_2(\cos k_x a_0 + \cos k_y a_0)],\end{aligned} \quad (2.5a)$$

$$\mathcal{J}_1(\vec{k}_\parallel) = 2J_1 S[\cos(\tfrac{1}{2}k_x a_0) + \cos(\tfrac{1}{2}k_y a_0)], \quad (2.5b)$$

and

$$\mathcal{J}_2(\vec{k}_\parallel) = SJ_2. \quad (2.5c)$$

For the spins in the first layer above the surface layer ($l_z = 1$), one finds

$$\begin{aligned}\Omega S(1) = {} & [\mathcal{J}_0(\vec{k}_\parallel) - \mathcal{J}_2(\vec{k}_\parallel)] S(1) \\ & - \mathcal{J}_1(\vec{k}_\parallel)[S(0) + S(2)] - \mathcal{J}_2(\vec{k}_\parallel) S(3),\end{aligned} \quad (2.6)$$

while for the surface spins we write

$$\Omega S(0) = \mathcal{J}_0^{(s)}(\vec{k}_\parallel) S(0) - \mathcal{J}_1(\vec{k}_\parallel) S(1) - \mathcal{J}_2(\vec{k}_\parallel) S(2), \quad (2.7)$$

where, with $J_1^{(s)} = r_1 J_1$ and $J_2^{(s)} = r_2 J_2$,

$$\begin{aligned}\mathcal{J}_0^{(s)}(\vec{k}_\parallel) = {} & S[4(1+r_1)J_1 + (4r_2+1)J_2 \\ & - 4r_1 J_1 \cos(\tfrac{1}{2}k_x a_0)\cos(\tfrac{1}{2}k_y a_0) \\ & - 2r_2 J_2(\cos k_x a_0 + \cos k_y a_0)].\end{aligned} \quad (2.8)$$

To study the surface spin waves associated with this geometry, we seek solutions of the system of equations above with

$$S(l_z) = S(0)\exp(-\tfrac{1}{2}q a_0 l_z). \quad (2.9)$$

The attenuation constant q may be related to the frequency Ω of the wave and to $\vec{k}_\parallel$ by inserting this form into Eq. (2.4). We demand that the real part of the attenuation constant q be positive always. Then from Eq. (2.4) we find

$$\Omega = \mathcal{J}_0(\vec{k}_\parallel) - 2\mathcal{J}_1(\vec{k}_\parallel)\cosh(\tfrac{1}{2}q a_0) - 2\mathcal{J}_2(\vec{k}_\parallel)\cosh(q a_0), \quad (2.10)$$

which allows us to solve for $\cosh(\frac{1}{2}q a_0)$:

$$\begin{aligned}\cosh(\tfrac{1}{2}q a_0) = {} & \frac{1}{4}\left(-\frac{\mathcal{J}_1(\vec{k}_\parallel)}{\mathcal{J}_2(\vec{k}_\parallel)} \pm \frac{1}{\mathcal{J}_2(\vec{k}_\parallel)}\right. \\ & \times\{\mathcal{J}_1^2(\vec{k}_\parallel) + 4\mathcal{J}_2(\vec{k}_\parallel) \\ & \left.\times[\mathcal{J}_0(\vec{k}_\parallel) + 2\mathcal{J}_2(\vec{k}_\parallel) - \Omega]\}^{1/2}\right).\end{aligned} \quad (2.11)$$

We are presuming here that the next-nearest-neighbor exchange $J_2 \neq 0$.

There are in general two values of q which emerge from Eq. (2.11). We shall see that one can always in fact find two values for which $\mathrm{Re}(q) > 0$. We call these two solutions q_+ and q_-, and we must superimpose the two in order to satisfy both Eq. (2.6) and Eq. (2.7). Thus, the wave function of the surface spin wave is given by

$$S(l_z) = S_+ \exp(-\tfrac{1}{2}i q_+ a_0 l_z) + S_- \exp(-\tfrac{1}{2}i q_- a_0 l_z). \quad (2.12)$$

We pause to comment on the nature of q_+ and q_-. Let $Q_\pm = q_\pm a_0$, and write Eq. (2.11) in the form

$$\cosh(\tfrac{1}{2}Q_\pm) = a \pm ib. \quad (2.13)$$

For the moment, we presume the quantity in the curly brackets in Eq. (2.11) is negative. If we write $Q_\pm = Q_\pm^{(1)} + iQ_\pm^{(2)}$, then Eq. (2.13) may be decomposed into

$$\cos(\tfrac{1}{2}Q_\pm^{(2)})\cosh(\tfrac{1}{2}Q_\pm^{(1)}) = a \quad (2.14a)$$

and

$$\sin(\tfrac{1}{2}Q_\pm^{(2)})\sinh(\tfrac{1}{2}Q_\pm^{(1)}) = \pm b. \quad (2.14b)$$

If we are given two numbers $Q_\pm^{(1)}, Q_\pm^{(2)}$ that satisfy Eqs. (2.14), then $-Q_\pm^{(1)}, -Q_\pm^{(2)}$ also are solutions. From this we see that we can always find two distinct solutions Q_+ and Q_- with $\mathrm{Re}(Q_+) > 0$ and $\mathrm{Re}(Q_-) > 0$, when the argument of the square root in Eq. (2.11) is negative. Furthermore, one has

$$Q_+ = Q_1 + iQ_2, \quad (2.15a)$$

$$Q_- = Q_1 - iQ_2. \quad (2.15b)$$

When the quantity in curly brackets in Eq. (2.11) is positive, again two values of Q may be found. Again we label them Q_+ and Q_-, although they may not be complex conjugates of each other.

If the form in Eq. (2.12) is inserted into Eq. (2.6) and it is noted that Eq. (2.10) is satisfied by both attenuation constants q_+ and q_-, one finds a constraint on the amplitudes S_+ and S_-:

$$\frac{S_+}{S_-} = -\frac{\sinh(\frac{1}{2}a_0 q_-)}{\sinh(\frac{1}{2}a_0 q_+)}. \tag{2.16}$$

Then if the solution is inserted into Eq. (2.7), after some algebra one finds

$$\frac{\sinh(\frac{1}{2}q_+ a_0)}{\sinh(\frac{1}{2}q_- a_0)} = \frac{\mathcal{J}_0(\vec{k}_\parallel) - \mathcal{J}_0^{(s)}(\vec{k}_\parallel) - \mathcal{J}_1(\vec{k}_\parallel)e^{q_+ a_0/2} - \mathcal{J}_2(\vec{k}_\parallel)e^{q_+ a_0}}{\mathcal{J}_0(\vec{k}_\parallel) - \mathcal{J}_0^{(s)}(\vec{k}_\parallel) - \mathcal{J}_1(\vec{k}_\parallel)e^{q_- a_0/2} - \mathcal{J}_2(\vec{k}_\parallel)e^{q_- a_0}}. \tag{2.17}$$

In general, for the model with next-nearest-neighbor exchange included, it is not possible to obtain a closed-form expression for the surface-spin-wave dispersion relation. However, the relations above allow one to compute the dispersion relation numerically with relative ease. One chooses a value of $\vec{k}_\parallel$, and searches for values of Ω (outside the bulk spin-wave frequency bands) which satisfy the above relations. One may do this by picking a value of Ω, computing q_+ and q_- from Eq. (2.11), then testing to see if Eq. (2.17) is satisfied.

There is a line in the two-dimensional Brillouin zone along which a closed solution emerges simply. This line is a key line for our stability considerations. Along the perimeter of the two-dimensional Brillouin zone illustrated in Fig. 2, we have that $\mathcal{J}_1(\vec{k}_\parallel) \equiv 0$. We concentrate here on the line between the points A and B in Fig. 2. Along this line,

$$k_x = (1/a_0)(2\pi - \theta), \tag{2.18a}$$

$$k_y = (1/a_0)\theta, \tag{2.18b}$$

where θ ranges from 0 to π. Then we have, with

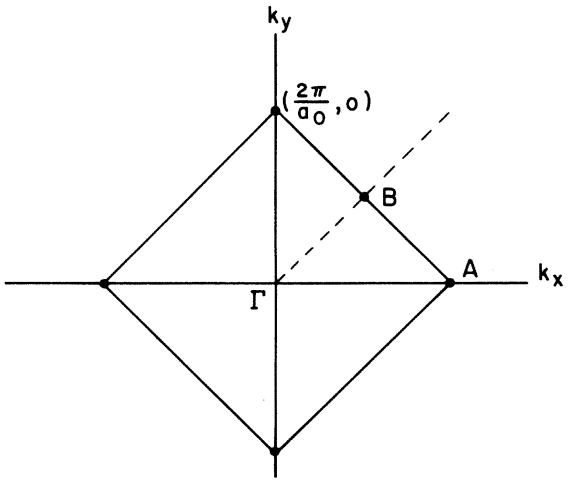

FIG. 2. Two-dimensional Brillouin zone for the fcc lattice with a (100) surface. The point B is the point $(\pi/a_0, \pi/a_0)$.

$$J_2 = -|J_2|,$$

$$\mathcal{J}_0(\vec{k}_\parallel) = 2S(7J_1 - 3|J_2|) + 2S(J_1 + 2|J_2|)\cos\theta, \tag{2.19a}$$

$$\mathcal{J}_1(\vec{k}_\parallel) = 0, \tag{2.19b}$$

$$\mathcal{J}_2(\vec{k}_\parallel) = -S|J_2|, \tag{2.19c}$$

and

$$\mathcal{J}_0^{(s)}(\vec{k}_\parallel) = S[2(2+3r_1)J_1 - (4r_2+1)|J_2| + (2J_1 r_1 + 4r_2|J_2|)\cos\theta]. \tag{2.19d}$$

With this form one finds

$$\tfrac{1}{2}q_+ a_0 = +\tfrac{1}{2}i\pi + K, \tag{2.20a}$$

$$\tfrac{1}{2}q_- a_0 = -\tfrac{1}{2}i\pi + K, \tag{2.20b}$$

where

$$\sinh(K) = \Delta \tag{2.21a}$$

and

$$\Delta = (1/2S^{1/2}|J_2|^{1/2})[\mathcal{J}_0(\vec{k}_\parallel) - 2S|J_2| - \Omega]^{1/2}. \tag{2.21b}$$

The combination $\mathcal{J}_0(\vec{k}_\parallel) - 2S|J_2|$ is the bottom of the band of bulk waves, with wave vector $\vec{k} = \vec{k}_\parallel + \hat{z}k_z$ for fixed $\vec{k}_\parallel$. The surface spin waves we consider have frequency lower than this value always, so the argument of the square root in Eq. (2.21b) is positive.

The values for q_+ and q_- in Eq. (2.20) allow the quantity $S(l_z)$ in Eq. (2.12) to be cast into the form

$$S(l_z) = S(0)(-1)^{l_z/2}e^{-Kl_z}, \quad l_z = 0, 2, 4, 6, \ldots, \tag{2.22a}$$

$$S(l_z) \equiv 0, \quad l_z = 1, 3, 5, \ldots; \tag{2.22b}$$

that is to say the spins in the odd numbered layers are not excited, and the spin motion is confined only to the even numbered layers.

After some algebra, the frequency $\Omega_s(\theta)$ of the surface spin wave along the line from A to B may be written

$$\Omega_s(\theta) = \Omega_m(\theta) - 4S|J_2|\eta(\theta)^2/[1 + 2\eta(\theta)], \tag{2.23}$$

where

$$\Omega_m(\theta) = 2S(7J_1 - 4|J_2| + J_1\cos\theta + 2|J_2|\cos\theta) \tag{2.24a}$$

is the minimum bulk spin-wave frequency described above, and

$$\eta(\theta) = (1/|J_2|)\{(5J_1 - 3|J_2| - 3r_1J_1 + 2r_2|J_2|) + [(1-r_1)J_1 + 2(1-r_2)|J_2|]\cos\theta\}. \tag{2.24b}$$

To obtain a surface spin wave, one must have $\eta(\theta) > 0$.

With the results above, we have studied the surface spin wave dispersion relation throughout the two-dimensional Brillouin zone, to search for values of the parameters that drive $\Omega_s(\vec{k}_\parallel)$ to zero. Before we present the results, we note that the bulk of the crystal is stable with respect to the ferromagnetic state whenever $|J_2| < J_1$. This criterion is obtained by requiring the bulk spin wave excitation energy to be positive always. Note that since there are six next-nearest neighbors and twelve nearest neighbors for the fcc lattice, the molecular-field theory admits ferromagnetic solutions for $|J_2|$ as large as $2J_1$. However, examination of the bulk spin-wave dispersion relation [obtained readily from Eq. (2.4)] shows that the bulk spin wave excitation energy becomes zero when $|J_2| = J_1$ at the point $\vec{k} = (\pi/a_0)(1, 1, 1)$. For larger values of $|J_2|$, the excitation energy is negative. Presumably this means the ferromagnetic state in the bulk is unstable with respect to an antiferromagnetic spin arrangement, and the ferromagnetic state is stable only for $|J_2| < J_1$.

Three dimensionless parameters enter the description of the model explored here. The first is $\epsilon = -|J_2|/J_1$, which as we just saw can change from 0 to -1 in value. The second two are r_1 and r_2. We have chosen in the interest of simplicity to scale both the nearest- and the next-nearest-neighbor exchange in the surface by the same factor, i.e., we take $r_1 = r_2 = r$. This restricted model includes the case where the exchange constants are unchanged near the surface ($r = 1$), and the model considered by Trullinger and Mills ($r < 0$, $\epsilon \equiv 0$).

For the case $r = 1$, in Fig. 3 we show the surface-spin-wave dispersion relation from the Γ point ($\vec{k}_\parallel = 0$) of the two-dimensional Brillouin zone along a straight line to the point B in Fig. 2. This is done for three values of ϵ. From Fig. 2, one sees that for $\epsilon = -0.8$, the excitation energy is positive definite. At the critical value $\epsilon = \epsilon_c$, where $\epsilon_c = \frac{1}{4}(\sqrt{57} - 11) = -0.86$, the dispersion curve just touches zero at the B point. For $-1 < \epsilon < \epsilon_c$, the excitation energy is negative near point B. A study of the dispersion relation shows that the dispersion curve first touches zero away from Γ at the B point when $\epsilon = \epsilon_c$.

This shows that when the surface exchange constants are unchanged from their values in the bulk, a ferromagnetic arrangement of the surface spins is unstable with respect to a reconstructed arrangement. A surface superlattice with the wave vector $\vec{k}_\parallel^{(B)}$ forms. We see from these considerations that Blandin's argument works in three dimensions, as well as in the semi-infinite plane of spins considered in his paper. We shall explore properties of the reconstructed surface spin configuration in Sec. III.

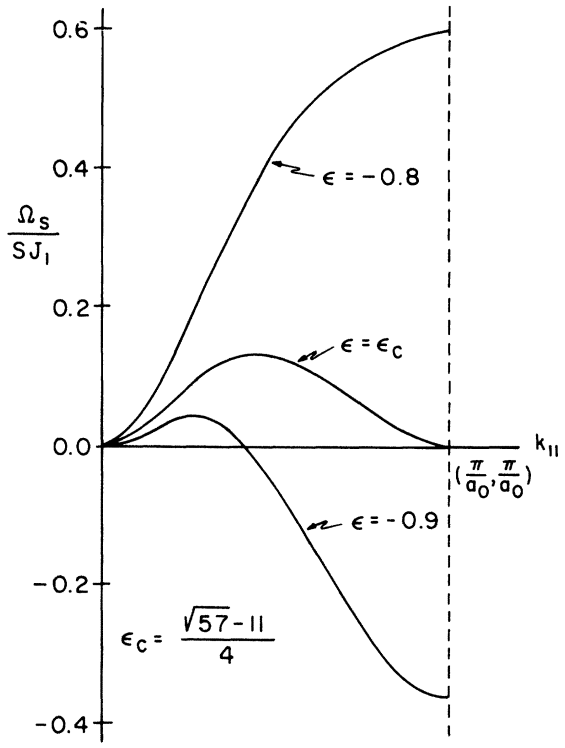

FIG. 3. Surface spin wave dispersion relation for the case $r_1 = r_2 = 1$, and various values of the parameter $\epsilon = -|J_2|/J_1$. For $\epsilon > \epsilon_c$, the surface wave excitation energy is positive, while for $-1 < \epsilon < \epsilon_c$, it becomes negative in the near vicinity of point B in Fig. 2.

By varying both ϵ and r, one may construct a phase diagram which shows the regions in the ϵ-r plane where the ferromagnetic arrangement of surface spins is stable, and where it is not. We have done this, and we find for all values of ϵ and r, the surface-spin-wave frequency always touches zero first at either point A or point B of Fig. 2. The results of this study are summarized in Figs. 4 and 5. In Fig. 4, the results for a wide range of r values are displayed. For large values of r, one might presume we have a description of a magnetic overlayer with strong exchange coupling on a more weakly interacting host spin system. We show in Fig. 4 the regimes of the parameter space where the surface frequency at the B point is negative, the A point is negative, or the frequency is negative at both. The boundary between the cross hatched regions and the unshaded region delineates the ranges of parameters for which the ferromagnetic surface spin configuration is stable. In Fig. 5, the same information is displayed for a more restricted range of r. This range may be more appropriate for a

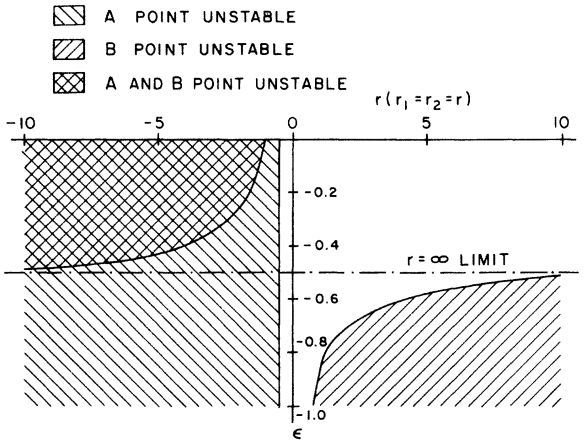

FIG. 4. Stability diagram for the surface region, in the ϵ-r plane. Results are displayed for a wide variation of the parameter r.

semi-infinite crystal with no overlayer present.

One sees from the information in Figs. 4 and 5 that the ferromagnetic surface spin arrangement is unstable for a rather wide range of parameters. With $r=1$ (surface exchange the same as the bulk), the B point instability occurs for a rather large value of $|J_2|/J_1$. If the surface exchange is stiffened ($r>1$), the critical value value of $|J_2|/J_1$ is lowered considerably. For example, it drops from 0.86 to roughly 0.7 when $r=2$. In addition, if near the surface, one does not have $r_1=r_2$, but rather $r_2>r_1$ by a considerable amount, the tendency toward the surface instability can be enhanced significantly. For example, if $r_1=1$ and $r_2=2$, then we find that the surface instability at the B point occurs at $|J_2|/J_1=0.467$. Thus,

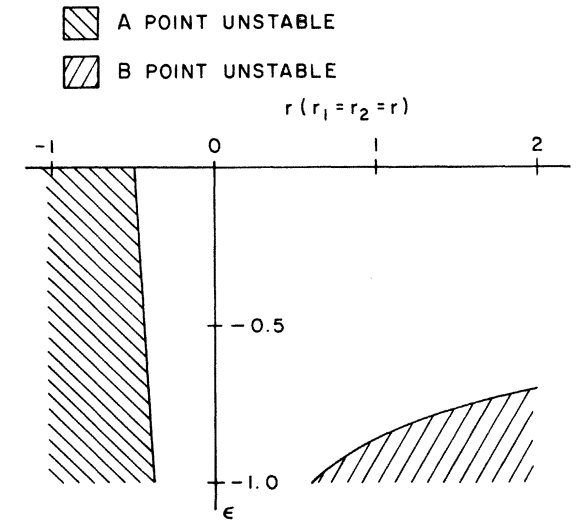

FIG. 5. Portion of the stability diagram displayed in Fig. 4 for $-1<r<2$.

by presuming $r_1=r_2$ in the interest of simplicity, we may have been led to underestimate the trend to surface spin instabilities. It would be most interesting to know what one would expect for values of the surface exchange interactions within the framework of theoretical investigations such as those described in Ref. 3.

This concludes our discussion of the stability of the ferromagnetic configuration in the surface at $T=0$. In Sec. III, we explore the temperature and field variation of the surface spin arrangement in mean-field theory.

III. NATURE OF THE RECONSTRUCTED SPIN CONFIGURATION

In Sec. II, we saw that the ferromagnetic arrangement of spins in the surface of our model ferromagnet is unstable with respect to a reconstructed spin configuration, for certain values of the model parameters. The method used in Sec. II can only delineate the phase boundary in the parameter space which separates the regime where surface ferromagnetism is stable at the absolute zero of temperature, and where it is not. The spin-wave theory is the magnetic analog of the harmonic approximation of lattice dynamics; anharmonic effects must be included before the new spin configuration can be found. In this section, we present an approximate description of the reconstructed spin arrangement and its dependence on magnetic field and temperature.

We shall base our discussion on the use of molecular-field theory. The application of molecular field theory to the semi-infinite ferromagnet[8] gives results in qualitative accord with those obtained from more rigorous considerations.[9] In the present case, we see that our interest will be primarily in the temperature region below the bulk Curie temperature. In this region, crudely speaking, the spins near the surface feel an effective exchange field from the aligned bulk spins that is strong. In conditions such as this, the use of mean-field theory seems reasonable.

We believe the results in the present section have pedagogical value that extends beyond the magnetic surface problems explored here. There have been recent lattice dynamical theories[10] which explore the stability of reconstructed atomic arrangements in and near the surface. These studies are the analog of the analysis in Sec. II, in that they explore a region of a parameter space to find where surface phonon excitation frequencies vanish. These lattice dynamical models are explored within the harmonic approximation, and to date no study of the displaced surface positions has been performed. The present discussion is a spin analog of how one might proceed with an

analysis of the atomic displacements in the reconstructed state.

We shall presume that in the reconstructed state, the spin arrangement near the surface has the same symmetry and nature as the eigenvector of the spin-wave mode which first goes soft. That is, in Figs. 4 and 5, we presume that if the parameters are such that the "system point" lies within the regime where the surface spin wave excitation energy is negative at the A point and positive at the B point, then the surface spin configuration is similar to a frozen in A point surface spin wave with macroscopic amplitude. Our task then is to find the temperature and magnetic field variation of the parameters which describe the surface spin arrangement.

In Fig. 6, we show the spin configuration in the surface layer, for both the A-point and B-point surface spin structures. In the numerical results presented in this section, we shall confine our attention to the case $r_1 = r_2 = 1$ and the B-point configuration, although the equations displayed allow r_1 and r_2 to differ from unity. We assume

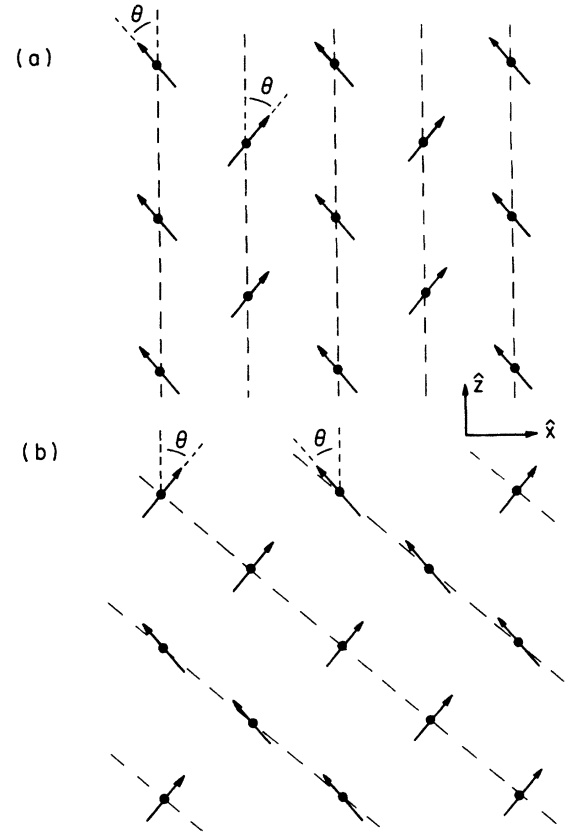

FIG. 6. Configuration of the surface spins in the region of (a) an A-point instability and (b) a B-point instability.

that in the surface, the angle between the spin and the $\hat{z}$ direction is θ_0.[11] The spins in the first layer inside the crystal are presumed perfectly aligned along $\hat{z}$, since the eigenvector in Eq. (2.22b) vanishes for $l_z = 1$. Indeed, we take θ_0, $\theta_2, \theta_4, \ldots$ to be nonzero, but $\theta_l \equiv 0$ for all odd l, as suggested by Eq. (2.22b).

We next write the equations of the molecular-field theory. There are two conditions that we impose, in contrast to the usual single self-consistent molecular-field equation. Suppose we imagine a given spin configuration characterized by the angles $\theta_0, \theta_2, \theta_4 \ldots$, and suppose in this spin configuration the expectation value of $\langle \vec{S} \rangle$ in layer l is a vector with magnitude $S\eta_l$, i.e., in layer l, we have

$$\langle \vec{S} \rangle_l = S\eta_l (\cos\theta_l \hat{z} \pm \sin\theta_l \hat{x}), \tag{3.1}$$

where the + sign is chosen for spins which lie on one of the two sublattices of Fig. 6, and the minus sign for those that lie on the second. Then for a given set of the η_l, and the angles θ_l, one can compute the molecular field $\vec{H}_\pm(\vec{l})$ felt by a spin on the plus or minus sublattice in layer $\vec{l}$. Then we have the usual equations of molecular field theory that must be satisfied. In the present case, these read

$$\eta_l = B_S\left(\frac{\mu \vec{S}_\pm(\vec{l}) \cdot \vec{H}_\pm(\vec{l})}{k_B T}\right), \tag{3.2}$$

where μ is the magnetic moment per spin, and we shall find $\vec{S}_+(\vec{l}) \cdot \vec{H}_+(\vec{l}) = \vec{S}_-(\vec{l}) \cdot \vec{H}_-(\vec{l})$. Here $B_S(x)$ is the Brillouin function

$$B_S(x) = (1 + 1/2S)\coth(S + \tfrac{1}{2})x - (1/2S)\coth(\tfrac{1}{2}x). \tag{3.3}$$

If the θ_l all vanish, then Eq. (3.2) may be used to solve self-consistently for the magnetization profile near the surface. This has been done in a number of papers, near T_C,[8] or at lower temperatures where the full Brillouin function must be used.[12] However, when the θ_l are nonzero, we have too many parameters and too few equations. One must impose the additional requirement that the torque on each sublattice vanish:

$$\vec{S}_\pm(\vec{l}) \times \vec{H}_\pm(\vec{l}) = 0. \tag{3.4}$$

This leads to further relations between the η_l and θ_l that supplement Eq. (3.2).

We illustrate the procedure outlined above, for the spin configuration illustrated in Fig. 6(b). We presume an external field is present and is parallel to the $\hat{z}$ axis. Its magnitude is H_0. A spin in the surface layer canted to the right in Fig. 6(b) (call this the "+" sublattice) feels the field $\vec{H}_+(0)$ given by

$$\mu\vec{H}_+(0)=\hat{z}\{\mu H_0+SJ_1[(4r_1+4\epsilon r_2)\eta_0\cos\theta_0 + 4\eta_1+\epsilon\eta_2\cos\theta_2]\} - \hat{x}SJ_1(4\epsilon r_2\eta_0\sin\theta_0+\epsilon\eta_2\sin\theta_2), \quad (3.5)$$

while in the first layer (recall $\theta_1=0$ so there is only a single sublattice in layer one)

$$\mu\vec{H}(1)=\hat{z}\{\mu H_0+J_1S[4\eta_0\cos\theta_0 + 4(1+\epsilon)\eta_1+4\eta_2\cos\theta_2+\epsilon\eta_3]\}. \quad (3.6)$$

For $l_y\geq 2$, in the even numbered layers the molecular field becomes

$$\mu\vec{H}_+(l_y)=\hat{z}\{\mu H_0+SJ_1[\epsilon\eta_{l_y-2}\cos\theta_{l_y-2}+4(\eta_{l_y-1}+\eta_{l_y+1})+4(1+\epsilon)\eta_{l_y}\cos\theta_{l_y}+\epsilon\eta_{l_y+2}\cos\theta_{l_y+2}]\} + \hat{x}SJ_1\epsilon(\eta_{l_y-2}\sin\theta_{l_y-2}+4\eta_{l_y}\sin\theta_{l_y}+\eta_{l_y+2}\sin\theta_{l_y+2}). \quad (3.7)$$

For odd-numbered layers with $l_y\geq 3$, $\vec{H}_+(l_y)$ is found from Eq. (3.6) with the replacements $\eta_0\to\eta_{l_y-1}$, $\eta_1\to\eta_{l_y}$, $\eta_2\to\eta_{l_y+1}$, $\eta_3\to\eta_{l_y+2}+\eta_{l_y-2}$, $\theta_0\to\theta_{l_y-1}$, and finally $\theta_2\to\theta_{l_y+1}$.

Consider the form assumed by the zero-torque condition in Eq. (3.4). For each layer, the application of the condition to the + and − sublattices leads to the same result. If the condition is applied to spins in the surface $l_y=0$, the result may be arranged to read

$$\sin(\theta_0+\theta_2)=-(4\sin\theta_0/\epsilon\eta_2)\times[\tfrac{1}{4}h+(r_1+2\epsilon r_2)\eta_0\cos\theta_0+\eta_1], \quad (3.8)$$

where

$$h=\mu H_0/SJ_1.$$

We will use an iterative method to find the solution of the system of equations generated from Eqs. (3.2) and (3.4). Note that if we begin with an initial guess for the η_l and θ_0, then θ_2 may be found from Eq. (3.8).

The zero-torque condition is satisfied identically in all the odd-numbered layers, and for $l_y\geq 2$, we have

$$\sin(\theta_{l_y+2}+\theta_{l_y})=-(1/\epsilon\eta_{l_y+2})[h+\epsilon\eta_{l_y-2}\sin(\theta_{l_y-2}+\theta_{l_y})+4(\eta_{l_y-1}+\eta_{l_y+1})\sin\theta_{l_y}+2(1+2\epsilon)\eta_{l_y}\sin 2\theta_{l_y}]. \quad (3.9)$$

Thus, for a given guess for the η_l and θ_0, the angles θ_{2l} within the interior consistent with these parameters may be generated from Eqs. (3.8) and (3.9).

We have proceeded by presuming that η_0–η_9 differ from their bulk values while η_l for $l\geq 10$ assumes the bulk value η_∞ obtained from mean-field theory applied to the bulk material. In a similar way, θ_0–θ_{10} were allowed to be nonzero, while θ_{2l} was taken identically zero for $l\geq 6$.

The iteration procedure was applied in stages, in a manner which allowed the above range of variables to be computed. First, an approximate value of θ_0 is required. If one chooses a value too far off the correct one, the iteration procedure leads to a sequence of θ_{2l} which diverge as $l\to\infty$. So we began by allowing η_0–η_5 only to differ from the bulk, and only θ_0, θ_2, θ_4, and θ_6 to differ from zero. The truncated equations were solved to convergence by repeated iteration, for one hundred values of θ_0 from 0 to $\frac{1}{2}\pi$. It was found that only within a narrow range $\Delta\theta_0$ around a particular value of θ_0 one had $\theta_6<\theta_4<\theta_2<\theta_0$, as expected from physical considerations. The procedure was repeated by allowing θ_0, θ_2, θ_4, θ_6, and θ_8 to differ from zero, along with η_0–η_7. This narrows the acceptable range of θ_0 still further, by use of the requirement $\theta_8<\theta_6<\cdots<\theta_0$. Successive iterations with an increasing number of unconstrained variables were carried out to the point where η_0–η_9 were allowed to differ from the bulk variables, as well as θ_0–θ_{10}. In all the calculations reported here, θ_{10} was found to be very small, and the difference between η_9 and η_∞ quantitatively insignificant.

In all the calculations reported here, we chose $r_1=r_2=1$, so then only $\epsilon=-|J_2|/J_1$, h, and the spin S are left as parameters. With the divalent europium ion in mind, we have taken $S=\frac{7}{2}$ always.

In Fig. 7 we plot the angle θ_0 as a function of temperature for $\epsilon=-0.9$ and $\epsilon=-0.95$ in zero magnetic field, and $\epsilon=-0.9$ in a magnetic field with $h\cong 0.28$. One sees that a surface phase transition occurs, with $\theta_0(T)\to 0$ as $T\to T_s$, a surface transition temperature lower than the bulk Curie temperature T_C. The results displayed in Fig.

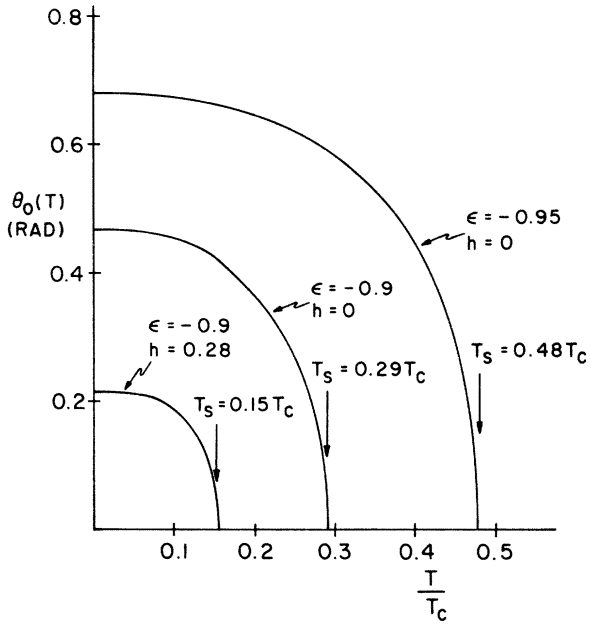

FIG. 7. Variation of the angle θ_0 with temperature, for $\epsilon = -0.9$ and $\epsilon = -0.95$. Here T_c is the bulk Curie temperature.

7 are all obtained from numerical calculations, so we do not have a closed expression for the critical exponent that characterizes the manner in which $\theta_0(T)$ vanishes. However, the results seem consistent with the square root variation of the order parameter that obtains in mean field theory, i.e., near T_s, $\theta_0(T) \propto (1 - T/T_s)^{1/2}$.

We see in Fig. 7 that application of a magnetic field depresses the value of $\theta_0(0)$ significantly, as expected on physical grounds. Furthermore, there is still a well defined surface phase transition in the field, with the surface transition temperature $T_s(H) < T_s(0)$.

We note that the magnetic field that corresponds to $h = 0.28$ is rather modest, if the bulk Curie temperature is not too high. For example, if $T_C = 20°$, $h = 0.28$ corresponds to an applied field of about 5 kG, for $S = \frac{7}{2}$. Thus, the reconstructed spin configuration is quite sensitive to applied magnetic field. Furthermore, there is a critical magnetic field $h_c^{(s)}$ which suppresses the surface phase transition. This may be seen by including an external field in the analysis of Sec. II.

In Fig. 8, we show the variation of the angle θ_l with distance from the surface. The calculations have been performed for $\epsilon = -0.9$ and $h = 0$. In Fig. 8(a), we show the results for $T = 0.1T_C$, a temperature low compared to the surface transition temperature T_s. In Fig. 8(b), we give results for $T = 0.287T_C$, a temperature quite close to T_s. One sees from these curves that the reconstructed spin arrangement remains confined to the near vicinity of the surface as $T \to T_s$. The physical reason for this is that the bulk correlation length remains short as long as T is well below the bulk Curie temperature T_C.

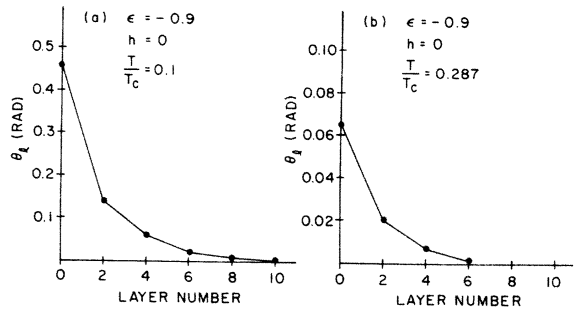

FIG. 8. Variation of the angle θ_l with distance from the surface, for the case $\epsilon = -0.9$ and $h = 0$. The calculations have been carried out for (a) $T = 0.1\,T_c$ ($T \ll T_s$) and (b) $T = 0.287\,T_C$ (close to T_s).

In Fig. 9, the variation of η with distance from the surface is displayed. In Figs. 9(a) and 9(b), we give results for $\epsilon = -0.9$ and $h = 0$, for the

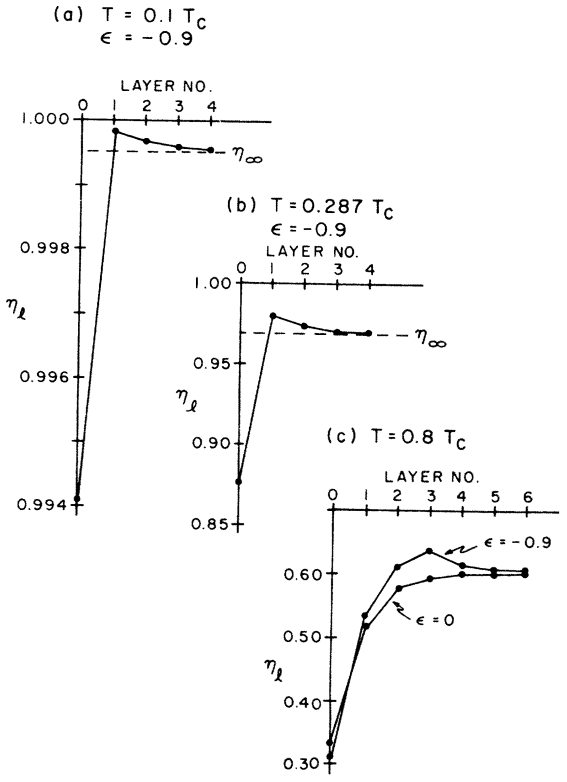

FIG. 9. Variation of η_l with distance from the surface. In (a) and (b) we show the results for $\epsilon = -0.9$, $h = 0$ for the temperatures $T = 0.1T_C$ and $T = 0.287T_C$, respectively. In (c), the result with $\epsilon = -0.9$ is compared to that with $\epsilon = 0$.

same two temperatures considered in Fig. 8. The parameters η_l differ appreciably from their bulk values only very near the surface. A striking feature present in these results is the appearance of a maximum in η_l just inside the surface, i.e., we always find that near the surface, η_l rises to a maximum value greater than η_∞. This effect occurs when antiferromagnetic next-nearest-neighbor exchange is present. We illustrate this in Fig. 9(c), where we compare curves calculated for $\epsilon = -0.9$ and $\epsilon = 0$. In the latter instance, there is no surface reconstruction. We have verified that the maximum in η_l has its origin in the presence of antiferromagnetic exchange rather than surface reconstruction by comparing curves with $\epsilon = -0.5$ (surface spins ferromagnetic) with $\epsilon = 0$. Again a maximum is found, although it is less prominent than that illustrated in Figs. 9(a) and 9(b).

We conclude with an expanded discussion of the effect of an external magnetic field on the surface spin arrangement. We see from Fig. 7 that θ_0 depends on h. Of course, all the θ_l's will be affected by the application of a field, as will the η_l's. If h is small, then we can introduce a set of susceptibilities by writing

$$\theta_l(h, T) = \theta_l(0, T) + \left(\frac{\partial \theta_l}{\partial h}\right)_0 h + \cdots \qquad (3.10a)$$

and also

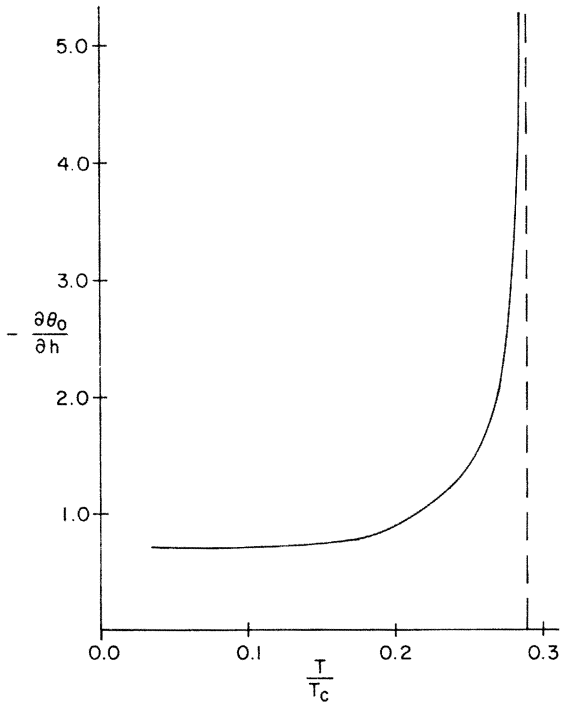

FIG. 10. Temperature variation of $(\partial \theta_0/\partial h)_0$ for $\epsilon = -0.9$.

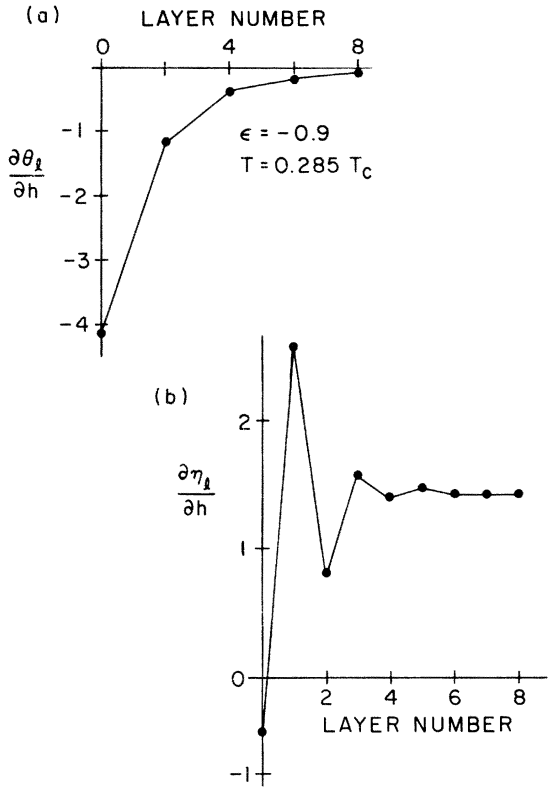

FIG. 11. (a) Variation of $(\partial \theta_l/\partial h)_0$ with layer number and (b) variation of $(\partial \eta_l/\partial h)_0$ with layer number. The calculations take $\epsilon = -0.9$, and $T = 0.285 T_C$, a temperature close to the surface transition temperature.

$$\eta_l(h, T) = \eta_l(0, T) + \left(\frac{\partial \eta_l}{\partial h}\right)_0 h + \cdots . \qquad (3.10b)$$

The susceptibilities introduced in Eq. (3.10) may be calculated in the following manner. The θ_l and η_l parameters are found by solving the set of nonlinear equations generated from the zero-torque condition, and the mean-field equation for η_l. In each equation, h appears explicitly. We may differentiate each equation with respect to h, and set h to zero when this is complete. This leads to a set of linear, inhomogenous equations for the $(\partial \eta_l/\partial h)_0$ and $(\partial \theta_l/\partial h)_0$. The coefficients may all be expressed in terms of the η_l's and θ_l's appropriate to the case $h = 0$. We shall not give the explicit form of these relations here, since the expressions are cumbersome and their derivation straightforward from the expressions displayed above.

In our case, where η_0–η_9 is allowed to differ from η_∞ as well as θ_0–θ_{10}, the generalized susceptibilities may be calculated by inverting a 15×15 matrix.

In Fig. 10, we plot the value of $(\partial \theta_0/\partial h)_0$ as a function of temperature, for $\epsilon = -0.9$. The di-

vergence in this quantity as $T \to T_s$ is evident. Again it is hard for us to extract a critical exponent from these numerical results. It is apparent that as $T \to T_s$, the restructured surface spin configuration becomes quite sensitive to field.

In Fig. 11, we show the magnitude and variation with distance from the surface for $(\partial\theta_l/\partial h)_0$, and $(\partial\eta_l/\partial h)_0$. This is done for $\epsilon = -0.9$ again, and the temperature $0.285T_C$, a value quite close to T_s. We see that although $(\partial\theta_0/\partial h)_0$ becomes large as $T \to T_s$, the susceptibility drops to zero within a few layers of the surface.

IV. CONCLUDING REMARKS

In this paper, we have shown that under certain conditions, the spin arrangement within the surface of a ferromagnet may have symmetry lower than that in the bulk of the material. We have explored this phenomenon for a particular model of a ferromagnetic crystal. Whether or not this "magnetic reconstruction" will occur in real crystals is hard to predict at this point, since we know little about the magnitude of exchange constants near the surface of magnetic crystals.

We do note that one could detect the reconstructed spin configuration described here through conventional low-energy-electron-diffraction (LEED) studies. It would not be necessary to use a spin-polarized electron beam for this purpose, since the presence of the magnetic reconstruction would give use to fractional order Bragg peaks well separated from the nonmagnetic Bragg peaks. (Actually, there would be some displacement of the nuclei in the presence of the magnetic surface reconstruction by virtue of the spin-phonon coupling terms in the Hamiltonian. The half-order Bragg peaks thus arise from the nuclear displacements, as well as from the magnetic coupling between the electron and the spin array.) We believe it would be of very considerable interest to carry out LEED studies of the surface of the europium chalcogenides, if this may be done at temperatures well below the bulk ordering temperature. This would provide a direct test of our conjecture that the magnetic surface reconstruction is responsible for the anomalies observed in the spin-polarized photoemission experiments. Even if our conjecture is not correct, we note that LEED studies of these surfaces at low temperatures should prove of very great interest, in view of the above-mentioned anomalies.

Finally, there is no reason to believe the phenomenon of magnetic surface reconstruction is confined to ferromagnets. In principle, it should occur in antiferromagnets also, although the conditions under which this may occur have not been examined to date.

---

*Supported by Grant No. AFOSR 76-2887 of the Air Force Office of Scientific Research, Office of Aerospace Research, U.S.A.F.

†Supported in part through an NSF Exchange Fellowship, 1975-1976. Present address: Université Louis Pasteur, Laboratoire de Structure Electronique des Solides, 4 Rue Blaise Pascal, 67000, Strasbourg, France.

[1]S. E. Trullinger and D. L. Mills, Solid State Commun. 12, 819 (1973).

[2]T. Wolfram and R. de Wames, Prog. Surf. Sci. 2, 233 (1972). These authors do not discuss the nature of the new ground state in detail. Indeed, the surface-spin arrangement illustrated in their Fig. 9 is incorrect, as we see from Ref. 1 and the present discussion.

[3]T. Kasuya, IBM J. Res. Dev. 14, 214 (1970); L. D. Falkovskaya and V. A. Sapozhnikov, Phys. Status Solidi B 71, 469 (1975).

[4]A. Blandin, Solid State Commun. 13, 1537 (1973).

[5]K. Sattler and H. C. Siegmann, Phys. Rev. Lett. 29, 1565 (1972); M. Campagna, K. Sattler, and H. C. Siegmann, AIP Conf. Proc. 18, 1388 (1974); Helv. Phys. Acta 47, 27 (1974).

[6]F. Meier, D. T. Pierce, and K. Sattler, Solid State Commun. 16, 401 (1975).

[7]See, for example, R. E. Dewames and T. Wolfram, Phys. Rev. 185, 720 (1969); D. L. Mills, Phys. Rev. B 1, 264 (1970).

[8]D. L. Mills, Phys. Rev. B 3, 3887 (1971).

[9]K. Binder and P. C. Hohenberg, Phys. Rev. B 6, 3461 (1972); 9, 2194 (1974).

[10]S. E. Trullinger and S. L. Cunningham, Phys. Rev. Lett. 30, 913 (1973); and Phys. Rev. B 8, 2622 (1973). Also see S. E. Trullinger, thesis (University of California Irvine, 1975) (unpublished).

[11]Figure 6 is drawn with the $\hat{z}$ direction parallel to the surface, while in Sec. II the z axis was normal to it. Here we presume the net magnetic moment is along $\hat{z}$ since this is conventional, and in Fig. 6, $\hat{z}$ is chosen to lie parallel to the surface for the sake of convenience in illustrating the spin configuration. Since the energy of the spin arrangement is left unchanged by a rigid rotation of the whole ordered spin array, we can imagine $\hat{z}$ normal to the surface as in Sec. II, but the spin arrangement is then less easy to illustrate in a figure.

[12]T. Wolfram *et al.*, Surf. Sci. 28, 45 (1971); T. Takeda and H. Fukuyama, J. Phys. Soc. Jpn. 40, 925 (1976); J. Schwartz, L. Schwartz, and H. Fukuyama (unpublished).